jet INTL JOURNAL OF ELECTRONICS AND TELECOMMUNICATIONS, 2011, VOL. 57, NO. 3, PP. 359–362
Manuscript received July 6, 2011; revised August 2011. DOI: 10.2478/v10177-011-0048-1

Pseudo-Noise Waveform Design Minimizing Range and Doppler Masking Effect

Janusz S. Kulpa and Jacek Misiurewicz

***Abstract*—Noise radar is a very promising technology offering advantages which cannot be achieved in classical radar systems. Unfortunately, it has also several disadvantages. One of the most significant is the masking effect, where strong objects raise the noise floor preventing detection of weak ones and significantly affecting dynamic range. In this article method of designing waveform with reduced noise floor is presented.**

***Keywords*—Noise radar, noise SAR, waveform design.**

I. Introduction

NOISE radars are becoming more popular due to increasing computers' computational power. The technology is not yet mature, but it is anyway very promising. One of most important advantages over classical radars is unambiguity both in time and frequency domain [1] [2]. Moreover, the noise radar is harder to jam and to detect. The most significant disadvantage of using continuously transmitted noise as sounding waveform is the masking effect, where the weak target echo hides below the noise floor from strong scatterer or direct leakage echo [3]. This can significantly decrease dynamic range of the system. The level of noise floor is Bt times below the main peak. Usually this time-bandwidth product cannot be extended due to physical limitation: in computational power, observation time and available RF circuits bandwidth.

One of the methods to overcome this problem is CLEAN method, where one extracts the strongest echo with the corresponding noise floor from the received signals [4]. The method could work iteratively, sequentially removing multiple echoes. It works well only when strong echoes could be separately distinguished. Moreover, the method has high computational complexity, since after single iteration the whole image must be recalculated.

The alternative approach is to use a pre-distorted sounding signal with the reduced noise floor in the area of interest in range and Doppler dimension.

II. Crossambiguity Noise Floor Reduction

The aim of the algorithm described below is to obtain waveforms with reduced noise floor around the main autocorrelation peak. An algorithm for cancellation the correlation noise floor in range dimension was presented in [5]. The similar results based on the minimization of autocorrelation matrix was presented in [6]. It is suitable for a stop-and-go SAR imaging, but for a radar that works on moving platform or is used to detect the moving objects, the area of noise floor cancellation should include both range and Doppler plane.

To obtain the noise floor free region the following steps are taken:

1) A vector of N samples of white complex Gaussian pseudo-noise is generated.
2) The ambiguity function (crosscorrelation of the signal with itself and its copies shifted in Doppler domain) in both range and Doppler plane is calculated.
3) A set of coefficients a_{kl} to minimise ambiguity function are calculated for each time- ($_k$) and frequency- ($_l$) shift in area of interest.
4) Time- and frequency-shifted copies, scaled by $a_{k,l}$ factor, are subtracted from the original pseudo-noise.

A. Mathematical Solution

The algorithm consists in minimizing the ambiguity function in given points by appropriate subtraction of shifted copies of original signal. We are assuming that if the points of optimization are close to each other, the ambiguity function near these points will be relatively low. The subtraction of the signal copies is given with formula (1)

$$x_o(n) = x(n) + \sum_k \sum_l a_{k,l} \cdot x(n-k) \cdot \exp\left(\frac{2\pi jnl}{N}\right) \quad (1)$$

where $x_o(n)$ is an N-point signal with lower ambiguity sidelobes obtained from $x(n)$. The effort in this approach is to calculate the a_{kl} factors. Let us consider the 4-point optimisation, for set of points (K,L), (K+1,L), (K,L+1), (K+1,L+1). The ambiguity function of x_o is given by formula (2).

$$R_{x_o}(K,L) = \sum \left(x_{0,0}(n) + \sum_{k=K}^{K+1} \sum_{l=L}^{L+1} a_{k,l} \cdot x_{k,l}(n) \right) \cdot \left(x_{K,L}(n) + \sum_{k=K}^{K+1} \sum_{l=L}^{L+1} a_{k,l} \cdot x_{K+k,L+l}(n) \right)^* \quad (2)$$

where * is complex conjugate operator, and

$$\begin{aligned} x_{k,l}(n) &= x(n-k) \cdot \exp\left(\frac{2\pi jnl}{N}\right) \\ R_x(k,l) &= \sum \left(x_{0,0} \cdot x^*_{k,l}\right) \end{aligned}$$

As one can see, it is a combination of ambiguity function of original signal in point (K,L), 8 terms of multiplied ambiguity function with a factors in first power and 16 terms of multiplied ambiguity function with a factors in second power.

J. S. Kulpa and J. Misiurewicz are with Warsaw University of Technology, Institute of Electronic Systems, Nowowiejska 15/19, 00-665 Warsaw, Poland (e-mails: J.Kulpa@stud.elka.pw.edu.pl, jmisiure@elka.pw.edu.pl).

As the algorithm is working on pseudo-noise signal, the ambiguity function sidelobes are Bt times below mainlobe and we expect the a_{kl} factors to be at the same order. Therefore, in (2) one can neglect the terms with a's in the second power. For the aim of the article, we will also neglect the terms with conjugate a factors from the second part of sum in (2) which gives us the approximation of ambiguity function (3).

$$R_{x_o}(K,L) = \sum \left(x_{0,0}(n) + \sum_{k=K}^{K+1} \sum_{k=L}^{L+1} a_{k,l} \cdot x_{k,l}(n) \right) \cdot x^*_{K,L}(n) \tag{3}$$

The equation above might be rewritten considering the autoambiguity function of the original signal, resulting in (4).

$$R_{x_o}(K,L) = R_x(K,L) + \sum_{o=0}^{1} \sum_{p=0}^{1} a_{K+o,L+p} \cdot R_x(-o,-p) \tag{4}$$

Similar equation might be written for points (K+1,L),(K,L+1) and (K+1,L+1). Solving the above set of equations under condition of $R_{x_o} = 0$ leads us to (5)

$$R_{mat} = \begin{bmatrix} M_x(0) & M_x(-1) \\ M_x(1) & M_x(0) \end{bmatrix} \cdot A_{mat} \tag{5}$$

where

$$A_{mat} = \begin{bmatrix} a_{K,L} \\ a_{K+1,L} \\ a_{K,L+1} \\ a_{K+1,L+1} \end{bmatrix},$$

$$R_{mat} = \begin{bmatrix} R_x(K,L) \\ R_x(K+1,L) \\ R_x(K,L+1) \\ R_x(K+1,L+1) \end{bmatrix}$$

and

$$M_x(l) = \begin{bmatrix} R_x(0,l) & R_x(-1,l) \\ R_x(1,l) & R_x(0,l) \end{bmatrix}$$

Solving (5) gives the searched values $a_{k,l}$. The results may be then applied to equation (1) to obtain the sounding waveform with desired ambiguity function.

Due to neglecting non-zero terms in (2), the desired ambiguity function will not be strictly equal to 0, but it will be lower than in not-optimized noise. The algorithm might then be iteratively applied until desired level of sidelobes is obtained.

B. Simulations

The algorithm was implemented in MATLAB environment. Currently developed version of algorithm does not consider conjugate $a_{k,l}$ factors neither the factors in second power. This is large simplification resulting in fast algorithm, but some of accuracy may be lost. The algorithm then may be used iteratively to reduce the noise floor to the desired level. The improvement is dependent on number of suppressed values and length of the signal. The considered signal length is 2^{16} samples and the ambiguity function was cleared in about 600 points. The improvement achieved is 5 dB per iteration (Fig. 1). The improvement per iteration ratio should raise when applying more precise algorithm which is not neglecting the conjugate $a_{k,l}$.

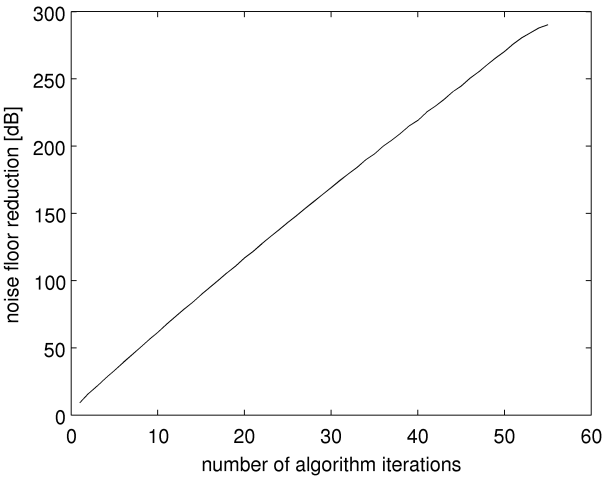

Fig. 1. The noise floor improvement depending on number of iterations.

Fig. 2 shows part of the ambiguity function of the waveform with reduced noise floor around the main correlation peak after 8 algorithm iterations. As one can see, the 65 dB improvement was achieved. The simulations showed that the ambiguity function of the modified pseudo-noise has symmetry properties (6), which should be taken into account when defining area of interest.

$$R_x(K,L) = R_x(-K,-L) \tag{6}$$

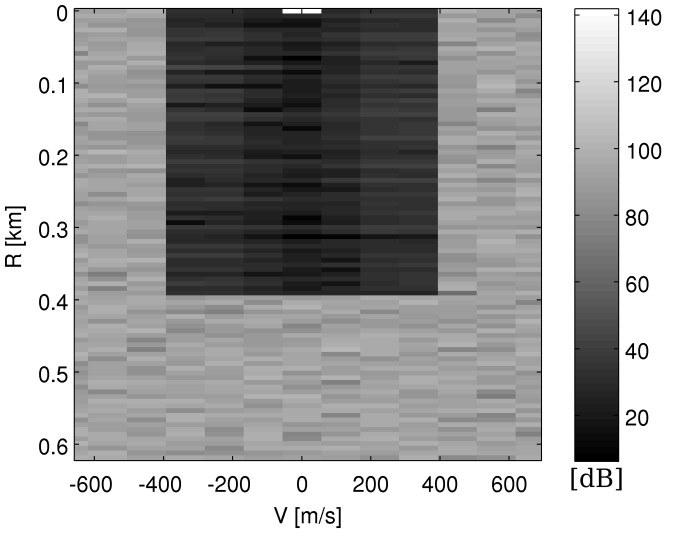

Fig. 2. The ambiguity function of one realization of designed waveform.

The ambiguity function of modified is almost equal to zero in the finite number of points in range-Doppler plane. In the

real-life condition we could not expect the integer delay of any target in the scene. When the cleared points are close to each other, it is believed that the ambiguity function between those points will not rise significantly.

III. Experimental Results

For verification of the theoretical approach, laboratory tests were conducted with real signals. As the source of the signal the Agilent's Arbitrary Waveform Generator(AWG) was used. The generator output signal was split by a -20 dB directional coupler. Both signals were connected to Vector Signal Analyser (VSA) (Fig. 3) by two cables of different lengths. The shorter one was used as reference signal, while the longer one was treated as echo signal. That simulates the scene with a single non-moving scatterer at the range corresponding to difference in cables length (Fig. 4). The analyser was synchronised to generator clock to avoid the clock drift. The parameters of the measurement were as follows.

- carrier frequency: 1.952 GHz
- transmitted power: 17.2 dBm
- sampling frequency: 46.08 MHz
- valid frequency span: 36 MHz
- number of correlated samples: 2^{16}

Fig. 3. The equipement used in the experiment.

After the measurements the crossambiguity function was calculated (Fig. 5). In the measurement about -10 dB of noise floor reduction was achieved. To achieve the best performance, the number of recorded samples should be equal to the length of generated signal. The difference between the noise floor reduction in simulation and measurements is result of the fractional delay of the signal and analogue filtering in the channel. Moreover, due to rectangular signal spectrum and

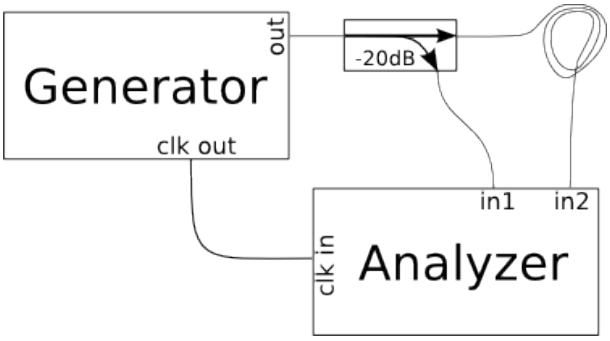

Fig. 4. The sketch of hardware setup.

envelope, the ambiguity function is convolved with the Sa function both in range and Doppler plane. This is clearly visible in correlation at zero Doppler shift.

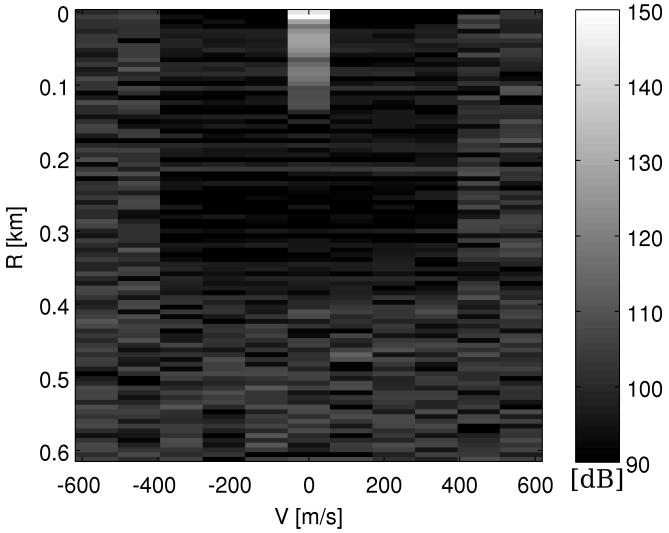

Fig. 5. The crossambiguity function of measured signals.

To fight the sidelobes, the windowing was applied. The spectrum of both reference and surveillance channel was shaped with the Hann window, while the time envelope was multiplied by Hamming window. As a result, the sidelobes were suppressed but the main lobe was broadened in both planes (Fig. 6). Applying window functions decreased the noise floor by 30 dB.

The cross-section of the ambiguity function of simulated signal, raw data and windowed data are shown in range for $v = 0\ m/s$ (Fig. 7) and in Doppler for $R = 0.27\ km$ (Fig. 8). The windowing suppresses the signal power, therefore the whole ambiguity function is shifted by 10 dB.

The test setup with the single delay line by the cable does not allow to measure the influence of Doppler shift in detail. To verify how the ambiguity function behaves when the signal is Doppler shifted by frequency which is fractional with respect to bin size, the recorded signal was digitally modulated (7).

$$y_{shift}[n] = y[n] \cdot e^{\frac{-j2\pi n \Delta f}{N}} \tag{7}$$

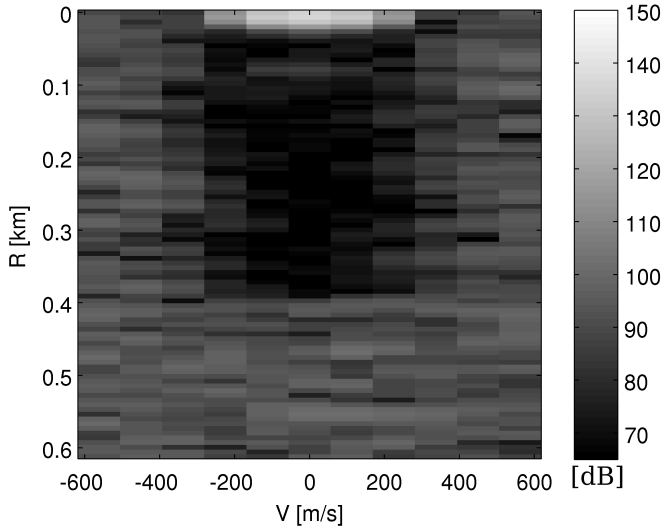

Fig. 6. The crossambiguity function of measured signals after windowing.

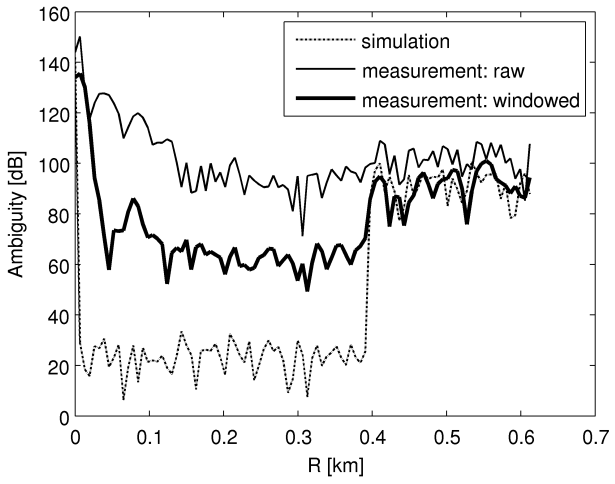

Fig. 7. The cross-section of ambiguity function for v=0 m/s.

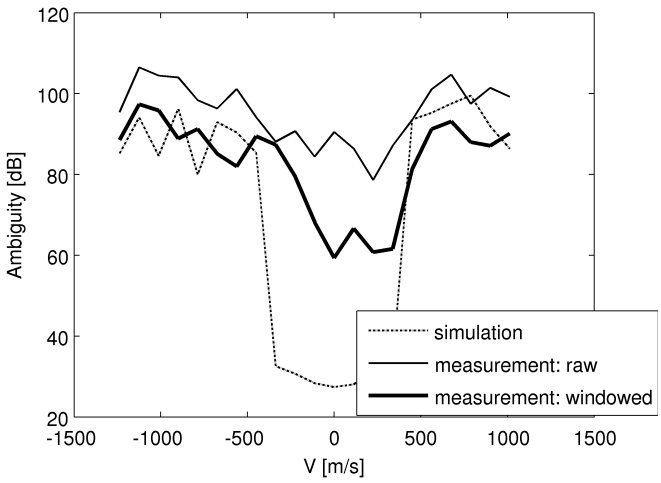

Fig. 8. The cross-section of ambiguity function for R=0.27 km.

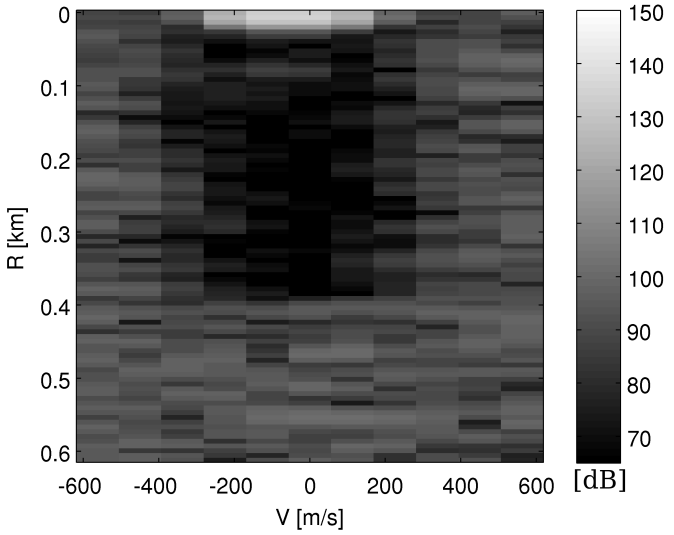

Fig. 9. The crossambiguity function with the frequency-shifted signal.

In simulation the signal was shifted by the half of Doppler bin and windowed both in time and frequency. The ambiguity function of the signal is shown in Fig. 9. The 25 dB of noise floor reduction was achieved.

IV. Conclusion

In this paper authors studied the algorithm for synthesis of pseudo-noise with reduced sidelobes in both range and Doppler plane in area of radar interest. The experiment with real-life signals was performed confirming the simulation results. A 30 dB improvement of cross-ambiguity function floor was achieved. This is equivalent of using the non-modified signal with 1000-times bigger time-bandwidth product.

Future work includes improving the algorithm to take into account part of previously neglected terms, reducing the amount of iteration required. Moreover, the inverse filters will be modelled to decrease influence of the analogue distortion in the channel.

The designed signals will be used in ground-based SAR experiments and Moving Target Detection.

References

[1] K. Lukin, A. Mogyla, V. Palamarchuk, P. Vyplavin, E. Kozhan, and S. Lukin, "Monitoring of St. Sophia Cathedral interior using Ka-band Ground Based Noise Waveform SAR," in *EuRAD 2009 – European Radar Conference*, Oct. 2009, pp. 215–217.

[2] K. Lukin, A. Mogyla, V. Palamarchuk, P. Vyplavin, O. Zemlyaniy, Y. Shiyan, and M. Zaets, "Ka-band bistatic ground-based noise waveform SAR for short-range applications," *Radar, Sonar Navigation, IET*, vol. 2, no. 4, pp. 233–243, Aug. 2008.

[3] K. Kulpa and Z. Czekala, "Short Distance Clutter Masking Effects in Noise Radars," *Applied Radio Electronics*, vol. 4, no. 1, pp. 96–98, 2005.

[4] K. Kulpa, K. Lukin, J. Misiurewicz, Z. Gajo, A. Mogila, and P. Vyplavin, "Quality enhancement of image generated with bistatic ground based noise waveform SAR," *Radar, Sonar Navigation, IET*, vol. 2, no. 4, pp. 263–273, Aug. 2008.

[5] J. Kulpa, L. Maslikowski, and K. Kulpa, "Pseudo-noise waveform synthesis for SAR applications," in *EuRAD 2010 – European Radar Conference*, Oct. 2010, pp. 25–28.

[6] P. Stoica, H. He, and J. Li, "New Algorithms for Designing Unimodular Sequences With Good Correlation Properties," *Signal Processing, IEEE Transactions on*, vol. 57, no. 4, pp. 1415–1425, Apr. 2009.